Mechanical properties of B-modified Ti-6Al-4V alloys

To cite this article: Indrani Sen 2010 *J. Phys.: Conf. Ser.* **240** 012039

Mechanical properties of B-modified Ti-6Al-4V alloys

Indrani Sen
Department of Materials Engineering, Indian Institute of Science
Bangalore 560 012, India

indrani@platinum.materials.iisc.ernet.in

Abstract. Minor addition of B to the Ti-6Al-4V alloy reduces the prior β grain size by more than an order of magnitude. TiB formed in-situ in the process has been noted to decorate the grain boundaries. This microstructural modification influences the mechanical behavior of the Ti-6Al-4V alloy significantly. In this paper, an overview of our current research on tensile properties, fracture toughness as well as notched and un-notched fatigue properties of Ti-6Al-4V-xB with x varying between 0.0 to 0.55 wt.% is presented. A quantitative relationship between the microstructural length scales and the various mechanical properties have been developed. Moreover, the effect of the presence of hard and brittle TiB has also been studied.

1. Introduction

Ti and its alloys are widely used in aerospace industries owing to their unique combination of low density and excellent mechanical properties such as strength and toughness. Among the Ti alloys, Ti-6Al-4V (referred hereafter as Ti64) is the most popular. In the as-cast condition, this alloy has grain size of the order of a few mm. Hence, expensive thermo-mechanical processing is employed to refine the microstructure where necessary. Recently it has been found that minor amount of B additions in the hypoeutectic range, markedly reduces the as-cast prior β grain size by an order of a magnitude [1]. For instance addition of 0.1 wt.% B reduces the grain size from ~ 1.7 mm to 150 μm [2]. Apart from the microstructural refinement, B addition to Ti64 alloy has significance in terms of producing in-situ TiB needles of width ~ 2-5 μm and aspect ratio ~ 10. Interestingly, TiB posses the appropriate balance of thermo-mechanical stability and similar thermal expansion co-efficient [3].

Since Ti64 is an aerospace grade alloy; its fracture and fatigue properties are of paramount importance from a designer's point of view. The present study was initiated to examine these in detail. This includes characterization of the elastic and plastic deformation behavior of the alloy under uniaxial tension, plane strain fracture toughness, fatigue crack growth and the un-notched fatigue behavior in terms of cyclic stress-strain curves as well as high cycle fatigue endurance limit. All these properties are rationalized in terms of microstructural modification that occurs due to B-addition to the Ti64 and TiB formation.

2. Materials and Experiments

Five grades of Ti-6Al-4V-xB alloys with x = 0.0, 0.04, 0.09, 0.30 and 0.55 wt.% are examined in this study. These alloys have been induction skull melted to achieve homogeneity in composition throughout the cast structure, followed by hot isostatic pressing at 900°C and 100 MPa pressure for two hours to reduce the cast porosity. Microstructural characterization of the alloys was performed on specimens that were metallographically polished and etched with Kroll's reagent.

Room temperature quasi-static tensile tests were performed on cylindrical dog-bone shaped specimens with 5 mm gage diameter and 25 mm gage length, subjected to a nominal strain rate of 0.001/s. Four specimens were tested for each composition. An extensometer of gage length 25 mm was mounted on the specimen surface to monitor the strains. Yield strength (σ_Y) and ultimate tensile strength (σ_U) as well as elastic modulus (E) were thus measured from the tensile tests. Ductility as measured by the elongation to failure, ε_f has also been recorded.

To characterize the cyclic stress-strain response, incremental step test (IST) method was utilized on highly polished dog-bone shaped specimens of gauge diameter and length 4.5 and 14 mm respectively. Maximum strain amplitude used was ± 1.0 or ± 1.2%. It has been found that a strain limit of ± 1.0 gives better stabilization. Highly polished hour glass shaped specimens of gauge diameter 4 mm are used for rotating-bending high cycle fatigue tests performed at a frequency of 100 Hz. 30-40 specimens were tested for each composition to obtain the endurance limit (EL) on the basis of a lifecycle of 10^7.

Fatigue crack growth experiments were performed on Chevron notched full C[T] specimens of width (W) 50 mm and thickness (B) 25 mm. The samples were fatigue pre cracked at a at constant cyclic load amplitude ΔP of 20,000N with the load ratio, R (minimum to maximum load) as 0.1. A frequency of 10 Hz is applied throughout the test with a sinusoidal waveform. After the precracking, the crack is grown further with the standard load-shedding method to determine the threshold stress intensity factor range (ΔK_0). Experimentally ΔK_0 is considered as the value of ΔK for which crack growth per cycle i.e. da/dN becomes less than 10^{-9} m cycle^{-1}. After reaching the ΔK_0, the specimens are observed in optical microscope to track the crack growth behavior in the near-threshold regime.

Plane-strain fracture toughness tests were performed after the initial precracking according to the ASTM standard procedure E399-90. For this, a crack opening displacement gage with a 2 mm travel is mounted on the knife edges, fixed on the specimens to measure the crack extension. Valid K_{IC} could not be achieved for Ti64-0.0B as well as Ti64-0.04B. However, for the rest of the B-modified alloys, K_{IC} is achieved. Fractography of the fatigue crack growth and fracture toughness specimens are done by scanning electron microscope to identify the fracture modes for the different alloys.

3. Results and Discussions

3.1.1. Microstructures

Representative microstructure of the B-modified alloys examined in this study is shown in Figure 1. It shows Widmanstätten structure with alternate lamellas of (hcp) α and (bcc) β oriented along particular directions within individual colonies. Such colonies are again distributed within the prior β grains. The TiB phase forms needle shaped particles of aspect ratio ~10 at the grain boundaries forming a necklace like arrangement. Prior β grain size (*D*) has been found to reduce by 96% with 0.55 wt.% B addition (Figure 2). Moreover, with B addition to Ti64, reductions in the aspect ratio of the laths as well as randomization of the colonies were also seen.

3.2. Tensile properties

Yield strength, σ_y, ultimate tensile strength, σ_u and tensile ductility, ε_f are determined from the quasistatic tensile stress-strain plots. Both σ_y and σ_u has been found to increase by 12-16% respectively with B addition (Figure 3). Interestingly this is found to be correlated to the inverse square root of grain size according to the Hall-Petch relation (Figure 4). However, E has been found to show a drastic enhancement with 0.04 wt.% B to Ti64, followed by a reduction. The overall E of the system has been found to increase linearly with B addition, except for 0.04 wt.% B addition [4]. On the other hand ε_f has been found to increase initially with up-to 0.09 wt.% B addition primarily due to drastic grain refinement (Figure 3). Further B additions, however produces higher volume fraction of hard TiB needles in the matrix and in turn reduces the global ductility of the system. Thus with 0.55

wt.% B addition, ε_f becomes almost similar to that of B-free alloy. In this sense, it seems practical to consider addition of ~0.1 wt.% B as the optimum amount of B that will give the highest benefits in terms of tensile properties.

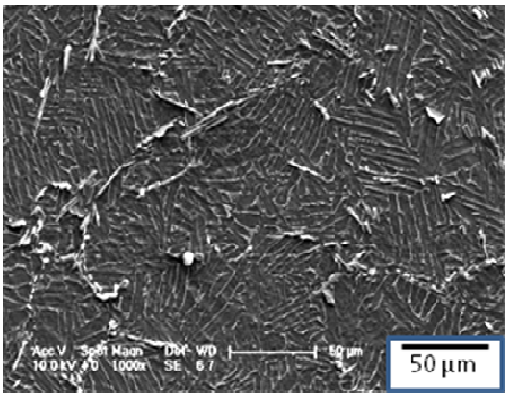

Figure 1. Representative scanning electron microstructure of Ti64-0.30B

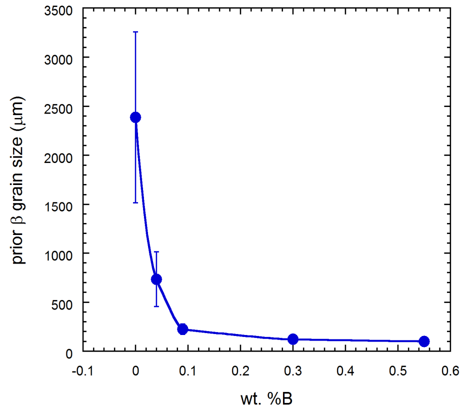

Figure 2. Variation of prior β grain size with B addition to Ti64.

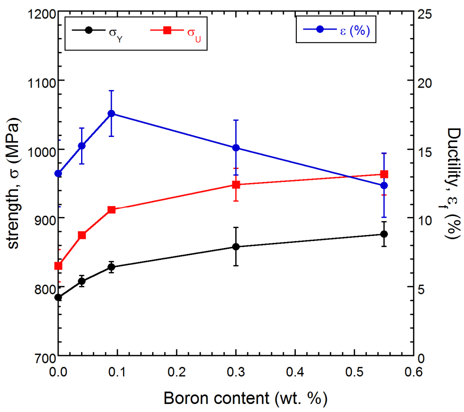

Figure 3. Variation of of σ_Y (MPa), σ_U (MPa) and ε_f (%) with B addition to Ti64.

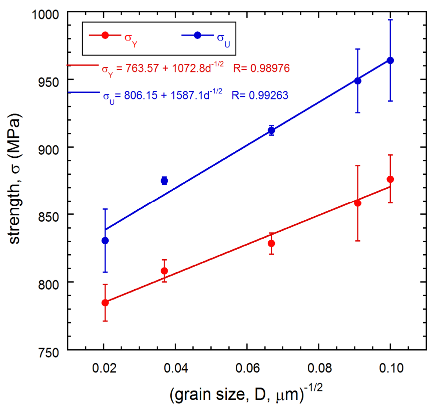

Figure 4. Variation of of σ_Y (MPa) and σ_U (MPa) with the inverse square root of grain size, *D*

3.3. Cyclic stress-strain

Cyclic softening is observed in all the alloys examined in this work. However, B modification has been found to increase the degree of softening. One possible reason could be the dislocation pile up at the α-β phase boundary, as well as dislocation-TiB particle entanglement. This activity in term will enhance the internal stress of the system. As a result, the applied stress necessary for further deformation will reduce and the material will soften cyclically. The more the amount of B is added, thicker will be the laths that can accommodate larger number of dislocation in a pile up and also larger will be the volume fraction of TiB and hence more will be the entanglement. Therefore cyclic softening has been found to increase with B addition to Ti64 [5].

3.4. High cycle fatigue

Endurance limit has been calculated from the high cycle fatigue experiments on the basis of limiting life of 10^7. It has been found that endurance limit increases with the increase in B addition to the system. This has been attributed to the grain size refinement with B addition. Since crack initiation is of prime importance for un-notched fatigue, it is the size of the grain that will have key role to play in controlling the endurance limit [5].

3.5. Fatigue crack growth

The values of ΔK_0 and the Paris exponent, *m*, for the alloys are calculated and ΔK_0 has been found to decrease with B addition up to 0.30B. However, a sudden increase is noted for the Ti64-0.55B alloy. Optical micrographs of fatigue crack near the threshold regime show that crack branching is a common feature for both the 0B and B-modified alloys. Deflection of the cracks by the lath boundaries as well as cutting the laths by the cracks to move forward on achieving higher stress concentration are other possible micro mechanisms, which enhance crack path tortuousity [2]. The crack path tortuousity was seen to decrease gradually with addition of B to Ti64. Since the crack path is trans-granular in nature, this can be related to the reduction of grain size. This is because of the fact that the growth of the crack gets arrested as the plastic zone size ahead of the crack tip reaches a critical microstructural size scale. A stress intensity factor range of the order of ΔK_0 is then needed to overcome the barrier and resume the crack growth. ΔK_0 is therefore directly related to the microstructural size of the alloy according to the relation ΔK_0 vs. $\sigma_Y{*}D^{0.5}$.

3.6. Fracture Toughness

Plane strain fracture toughness, K_{IC} (K_Q for 0.0B and 0.04B) has been found to decrease sharply by 66% with 0.55 wt.% B addition to Ti64. It is evident that with B addition, the resistance of Ti64 to fracture in the presence of a sharp crack and under severe tensile constraint decreases markedly. K_{IC} is thus believed to represent lower bound value of fracture toughness. According to RKR model [6], K_{IC} is directly proportional to σ_Y and a microscopic size parameter according to the following relation.

$$K_{IC} \propto \sqrt{D \times \sigma_y}$$

This relation shows a very good correspondence with a value of 0.99. Since with B addition, the increment in σ_y is only 12 % in comparison to the reduction in *D* by 96%, microstructural refinement is found to dominantly control the fracture toughness of the alloy. However, although B appears to be detrimental in terms of fracture resistance of Ti64, a value of 56 MPa $m^{1/2}$ is obtained for 0.09 wt.% B which is still in practical application limit and hence 0.1 wt.% B can be considered optimum to get maximum grain refinement, strength increment as well as ΔK_0 and K_{IC} still in applicable limit.

4. Conclusions

B addition to as cast-Ti64 causes significant grain refinement by an order of magnitude. This leads to enhancement in strength, ductility and elastic modulus as well as endurance limit. Degree of cyclic softening also increases with B addition. However, fracture toughness and fatigue threshold stress intensity factor range get reduced due to grain refinement. Considering all the above properties, it seems 0.1 wt.% B to Ti64 should be optimum in reducing the grain size to the maximum limit, enhancing strength and ductility while possessing the fracture and fatigue parameters within the practical application limits.

5. References

[1] Tamirisakandala S, Bhat R B, Tiley J.S and Miracle D B 2005 *Scripta Mater.* **53** 1421
[2] Sen I, Tamirisakandala S, Miracle D B and Ramamurty U 2007 *Acta Mater.* **55** 4983
[3] Sen I, Maheshwari L, Tamirisakandala S, Miracle D B and Ramamurty U 2009 *Mater. Sci. Eng. A* **518**; 162
[4] Sen I and Ramamurty U (2009) *submitted to Scripta Mater.*
[5] Sen I unpublished Ph.D thesis work
[6] Ritchie R O, Knott J F and Rice J R 1973 *J. Mech. Phys. Solids* **21** 39